

Spectroscopic and Photometric Observations of Unidentified Ultraviolet Variable Objects in GUVV-2 Catalog

Li, Y^{1,2}, Wang, J², Wei, J. Y.² and He, X. T.¹

¹ Department of Astronomy, Beijing Normal University, Beijing, 100875, China;
ollie-321@hotmail.com

² National Astronomical Observatories, Chinese Academy of Sciences, Beijing 100012, China

Received [year] [month] [day]; accepted [year] [month] [day]

Abstract An NUV-optical diagram made for sources from the second *Galaxy Evolution Explorer* (*GALEX*) Ultraviolet Variability (GUVV-2) Catalog provide us a method to tentatively classify the unknown GUVV2 sources by their NUV-optical magnitudes. On the purpose of testing the correctness and generality of the method, we carry out a program on the spectroscopic observations of the unidentified GUVV2 sources. The spectroscopic identification for these 37 sources are 19 type -A to -F stars, 10 type -G to -K stars and 7 M dwarf stars together with an AGN. We also present the light curves in R-band for two RR Lyrae star candidates selected from the NUV-optical diagram, both of which perform cyclic variations. Combining there light curves and colors, we classify them as RR Lyrae stars. To confirm the results, we shows a color-color diagram for the 37 newly spectroscopically identified objects compared with the previously identified ones, which manifests good consistence with our former results, indicating that the ultraviolet variable sources can be initially classified by their NUV/optical color-color diagram.

Key words: stars: variables: general — galaxies: active — methods: observational — ultraviolet emission

1 INTRODUCTION

The NASA *Galaxy Evolution Explorer* (*GALEX*) satellite (Martin et al. 2005) is an ongoing mission with the goal to study star formation in galaxies and its evolution with time in ultraviolet bands. A modified Ritchey-Chretien telescope with diameter of 50 cm and field-of-view of 1.2° is used to image and spectroscopically observe sky in two ultraviolet bands (NUV 1750–2750 Å, FUV 1350–1750 Å) down to an AB magnitude of $m_{AB} \sim 25$ in the deepest modes (Morrissey et al. 2007). It has totally imaged $2/3$ sky¹ during its All-sky Imaging Survey (AIS) and during its Medium Imaging Survey (MIS) and Deep Imaging Survey (DIS) since the launch on 2003 April 28.

Repeated observations of selected areas of the sky enabling numerous sources to have their FUV and NUV fluxes to be determined at many different epochs. Thus, the variable ultraviolet sources can be detected and many of which exhibit much larger amplitudes of variation in the ultraviolet region than that typically found at visible wavelengths (Wheatley et al. 2008).

In addition to the shallow survey, *GALEX* repeatedly performed the deeper image observations for the selected sky area. The repeat observations in DIS and MIS allow Welsh et al. (2005) released the first

¹ The *GALEX* pointings are kept away from the Galactic plane and Magellanic clouds in order to avoid the damage of its detector caused by the bright stars (~ 10 th magnitude)

GALEX ultraviolet variability catalog (GUVV1), which contains 84 variable and transient UV sources obtained during the first 15 months of the *GALEX* all-sky imaging survey. M dwarf flare stars and ab-type RR Lyrae stars are the largest ultraviolet variable objects detected by *GALEX* in GUVV1 (Welsh et al. 2005). The sample is subsequently enlarged to the second version (GUVV2, Wheatley et al. 2008) by the repeated observations in DIS and in certain Guest Investigator (GI) observations. GUVV2 contains 410 variable sources obtained during the period 2003 June - 2006 June. About 72% sources in GUVV2 had not been spectroscopically identified at that time. The already identified objects by SIMBAD catalog in GUVV2 are mainly quasars/AGNs (77), RR Lyrae stars (6), dMe stars (2) and X-ray binaries (19).

We systematically performed follow-up optical spectroscopic and photometric observations for the unknown sources listed in the GUVV2 catalog.

In this paper, we provide a method to tentatively classify ultraviolet variable sources into several common source types by their NUV-optical color-color diagram. This method is confirmed by our spectroscopic and photometric observations. We report results of the spectroscopic identification for 37 previously unknown sources and photometric monitors carried out for two unidentified RR Lyrae star candidates to confirm their variability through their light curves. The paper is organized as follows. §2 presents the motivations, observations and data reductions. The results and discussions are given in §3 and §4, respectively, and followed by the conclusion.

2 MOTIVATIONS, OBSERVATIONS AND DATA REDUCTION

2.1 Motivations

In GUVV2, of the 114 sources with previous SIMBAD catalog identifications, there are three mainly common types: quasars/AGNs, RR Lyrae stars, M dwarf stars. In order to statistically analyze the spectral types of GUVV2 sources, we have produced a color-color diagram for them by using their NUV magnitudes and optical magnitudes of B2 and R2 from USNO-B1.0 catalog (Monet et al. 2003) (Fig. 1). The sources contained in this diagram are previously known quasars/AGNs, RR Lyrae stars, M dwarf stars and the unidentified ones. The plot of (NUV_{max} -B2) versus (B2-R2) magnitudes reveals that the sources are segregated into different isolated regions according to their spectral types. The AGNs are mainly clustered at the bottom-left corner because of their non-thermal blue spectrum and strong NUV emission from the hot disk around the central supermassive black hole. The RR Lyrae stars are located within the region at right of the AGNs because of the strong Balmer jumps. The M dwarf stars are located at the top-right end of the diagram simply because of their low stellar surface temperature. The distribution of these previously known sources allows us to classify the unknown sources simply by their NUV-optical colors in advance.

To preliminarily test the results, we have chosen two RR Lyrae star candidates from the region where RR Lyrae stars locate to perform photometric monitors. These two sources are also selected as RR Lyrae star candidates by their SDSS magnitudes (Wheatley et al. 2008).

Taking account of the poor sample of the GUVV2-SIMBAD crossed sources and their potential bias, we have performed further spectroscopic observations for the randomly chosen unknown sources in GUVV2 to verify the correctness and generality of this method.

2.2 Spectroscopic observations

We only carried out the spectroscopic observations for the unidentified GUVV2 sources with B-band magnitude brighter than 17.5 magnitude and declination $> -15^\circ$ due to the constraint of the observatory site and the instrumental capability. Basing on the limitation of our observing time, sources were chosen according to their suitable right ascension in every run of our observations. This principle results in a list of 37 unidentified sources to be observed (Table 1.).

The spectroscopic observations were performed in several observing runs between 2009 and 2010 by using the National Astronomical Observatories, Chinese Academy of Sciences (NAOC) 2.16m telescope in Xinglong Observatory. The observations were taken with the OMR spectrograph attached at the

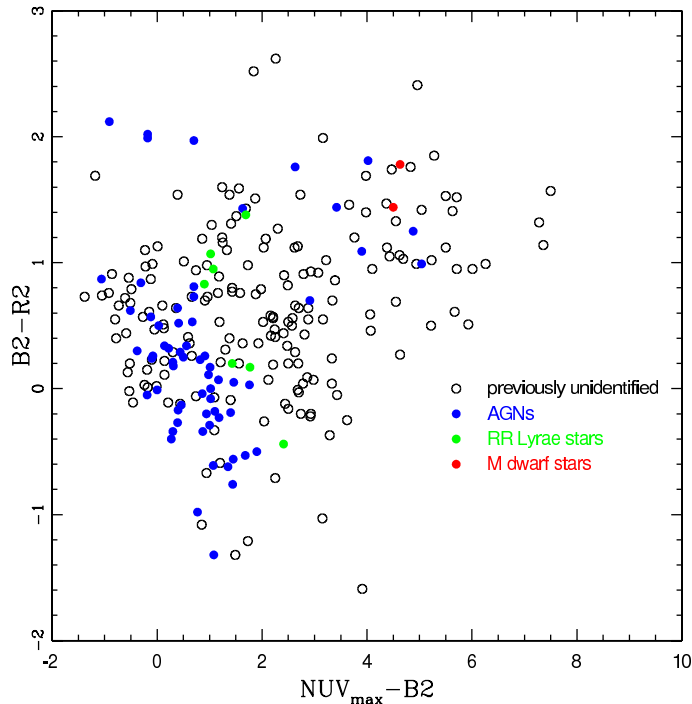


Fig. 1 Plot of $(NUV_{max} - B2)$ vs. $(B2 - R2)$ for previously identified variable sources. The filled circles with colors of blue, green and red are previously identified AGNs, RR Lyrae stars and M dwarf stars, respectively. The black open circles have no current identifications.

Cassegrain focus, and a back-illuminated SPEC10 1024×400 CCD camera employed as the detector. A grating of 300 g mm^{-1} and a slit of around $2''.0$ oriented in the south-north direction were used. This setup results in a final spectral resolution of $\sim 9\text{\AA}$ as measured from both comparison spectra and night sky emission lines. The spectroscopic observation log for the identified objects was listed in Table 1.

The wavelength calibrations were carried out by the He/Ne/Ar comparison arcs taken several times in each observation run. Two or three Kitt Peak National Observatory (KPNO) standard stars (Massey et al. 1988) were observed per night for flux calibration.

The raw data were bias subtracted, flat-field corrected, and cosmic-rays removed by using the IRAF package². The one-dimensional sky-subtracted spectra were then wavelength and flux calibrated. The uncertainties of the wavelength and flux calibrations are no more than 1\AA and 20%, respectively.

2.3 Photometric observations

To confirm the results, on the basis of our observing time, we have chosen two unidentified RR Lyrae star candidates from the region where RR Lyrae stars locates on the NUV-optical diagram with suitable brightness and right ascension to perform photometric monitors. These two sources (GALEX J100133.2+014328.5 and GALEX J155800.6+535233.6) are also selected as RR Lyrae star candidates by their SDSS magnitudes (Wheatley et al. 2008). Each of the two sources was monitored by using the 85cm NBT telescope at Xinglong Observatory of NAOC for two days from 2010 March 09 to 2010 March 10. A standard Johnson-Cousin-Bessel system is mounted on the primary focus of

² IRAF is distributed by the National Optical Astronomy Observatory, which is operated by the Association of Universities for Research in Astronomy, Inc., under cooperative agreement with the National Science Foundation; <http://iraf.noao.edu>.

Table 1 The Observation Log For The identified Objects

GALEX ID (1)	α (J2000.0) (2)	δ (J2000.0) (3)	N_{det} (4)	NUV_{max} (5)	ΔNUV (6)	$B2$ (7)	$R2$ (8)	I (9)	Obs.Date (10)	Exposure (sec) (11)	Spectral Type (12)
GALEX J002442.4+165808.0	00 24 42.52	+16 58 06.4	8	17.68	0.71	13.62	13.03	12.67	Oct. 14 2009	900	F
GALEX J004215.3+200957.3	00 42 15.36	+20 09 59.8	15	18.94	1.65	13.88	12.35	11.08	Oct. 14 2009	900	G
GALEX J013642.0-062743.1	01 36 42.03	-06 27 43.8	10	19.70	0.63	16.79	16.31	16.12	Oct. 14 2009	2400	A
GALEX J021547.1-045207.8	02 15 47.14	-04 52 08.2	7	19.60	0.67	15.06	12.96	12.37	Sep. 21 2009	900	G
GALEX J022003.0-032910.7	02 20 03.08	-03 29 10.1	7	20.01	0.73	16.19	14.44	13.77	Oct. 14 2009	1800	K
GALEX J022050.6-061528.0	02 20 50.71	-06 15 28.4	7	18.99	0.77	14.67	13.14	12.24	Sep. 21 2009	900	G
GALEX J042733.6+165222.2	04 27 33.67	+16 52 21.8	5	20.18	0.73	16.34	14.90	12.93	Jan. 23 2010	900	M
GALEX J042832.3+165821.6	04 28 32.37	+16 58 21.2	7	19.30	1.64	16.60	15.96	14.90	Jan. 23 2010	1800	F
GALEX J043431.2+172220.1	04 34 31.28	+17 22 20.2	13	19.66	0.71	17.22	15.05	14.36	Jan. 25 2010	2400	M
GALEX J081226.4+033320.5	08 12 26.37	+03 33 20.4	77	18.95	1.95	17.26	15.88	16.00	Jan. 25 2010	3600	F
GALEX J090853.4-021242.8	09 08 53.48	-02 12 43.2	13	19.23	0.98	15.90	15.66	16.16	Nov. 10 2010	3600	F
GALEX J091332.6-101108.2	09 13 32.65	-10 11 08.1	15	19.11	1.47	15.35	14.15	13.46	Nov. 10 2010	2400	AGN
GALEX J095847.6+021815.3	09 58 47.64	+02 18 15.1	11	18.62	1.42	14.59	13.54	13.03	Mar. 12 2010	1200	F
GALEX J102841.9+570840.4	10 28 41.94	+57 08 40.1	24	18.27	1.26	14.01	12.85	12.49	Mar. 15 2010	900	G
GALEX J102911.8+575806.1	10 29 11.81	+57 58 05.5	18	19.54	1.13	11.52	9.78	8.96	Mar. 15 2010	600	M
GALEX J102538.2+581549.1	10 25 38.19	+58 15 49.2	20	15.53	1.92	13.59	12.96	12.24	Mar. 15 2010	700	A
GALEX J120519.8-075605.6	12 05 19.83	-07 56 06.1	31	19.63	1.19	15.20	13.41	12.58	Mar. 13 2010	1200	K
GALEX J123523.7+614132.4	12 35 23.71	+61 41 31.9	92	20.34	0.61	14.50	13.48	12.84	Mar. 13 2010	900	K
GALEX J123718.3+624207.9	12 37 18.39	+62 42 07.9	29	20.23	0.75	13.89	12.18	10.81	Jan. 23 2010	2400	M
GALEX J132602.6+273502.3	13 26 02.68	+27 35 02.1	70	17.40	3.33	14.66	12.10	10.55	Jan. 23 2010	1800	M
GALEX J143126.4+342710.3	14 31 26.36	+34 27 10.4	18	18.40	0.86	13.78	12.72	11.68	Mar. 15 2010	600	G
GALEX J145110.3+310639.8	14 51 10.45	+31 06 40.7	24	18.72	0.86	13.58	11.24	9.78	Mar. 15 2010	600	M
GALEX J160902.8+524224.4	16 09 02.81	+52 42 24.4	18	19.11	0.74	17.36	18.00	17.44	Oct. 05 2010	3600	A
GALEX J163853.2+413932.7	16 38 53.25	+41 39 36.1	29	19.97	1.02	12.33	11.34	10.93	Oct. 06 2010	300	K
GALEX J163952.7+420951.6	16 39 52.77	+42 09 52.0	19	18.29	1.75	15.79	15.95	15.64	Oct. 05 2010	1200	A
GALEX J171250.9+582748.6	17 12 50.87	+58 27 48.4	14	18.51	0.63	16.06	15.74	15.40	Oct. 06 2010	900	A
GALEX J172033.4+585513.2	17 20 33.51	+58 55 13.5	37	20.12	0.80	15.12	14.34	14.13	Oct. 06 2010	900	G
GALEX J194443.4-074959.5	19 44 43.40	-07 49 59.4	11	19.85	0.76	15.08	12.90	11.36	Sep. 20 2009	600	M
GALEX J194704.9-075446.1	19 47 04.99	-07 54 47.0	7	19.56	1.43	16.78	16.74	16.32	Jun. 30 2009	1800	F
GALEX J203922.4-010346.0	20 39 22.45	-01 03 46.1	19	16.88	0.81	14.54	14.04	13.39	Sep. 21 2009	600	A
GALEX J203958.8-010714.3	20 39 58.85	-01 07 14.6	19	18.43	1.20	16.33	14.93	14.36	Oct. 06 2010	1200	F
GALEX J204024.3-010950.0	20 40 24.30	-01 09 50.7	15	19.06	0.72	16.53	16.29	15.35	Jun. 30 2009	1800	F
GALEX J204114.7-005220.9	20 41 14.80	-00 52 21.0	19	19.59	1.38	17.69	16.50	15.96	Jun. 30 2009	1800	F
GALEX J214909.5-050558.6	21 49 09.51	-05 05 59.1	26	18.67	2.28	17.29	16.89	16.50	Oct. 13 2009	2400	F
GALEX J223601.0+134711.5	22 36 01.10	+13 47 11.2	27	19.16	0.91	16.78	16.00	14.59	Oct. 06 2010	2400	A
GALEX J224029.0+120056.3	22 40 29.01	+12 00 55.7	19	17.56	0.85	15.73	14.59	14.37	Oct. 05 2010	1200	A
GALEX J224143.6+115326.2	22 41 43.67	+11 53 25.4	14	17.08	1.27	14.27	14.18	13.91	Oct. 14 2009	1200	A

Notes: Column (2)-(3) list the right ascension (J2000.0) and corresponding declination (J2000.0) of the objects given by 2MASS except GALEX J160902.8+524224.4 given by SDSS, column(4) lists the total number of detections (NUV_{det}) of the variable sources, column (5) lists the maximum NUV magnitude for the source (measured in a single exposure) and column (6) lists the variation between the corresponding maximum and minimum NUV magnitudes, column (7)-(9) list the photometric magnitudes of B2, R2 and I given by USNO-B1.0

the telescope. A PI1024 BFT 1024 \times 1024 CCD is used as the detector. The field-of-view is about 16.5×16.5 arcmin² at a focal ratio of 3.27 ($f=2780$ mm), which results in an image scale of 0.96 arcsec per pixel (Zhou et al. 2009). The standard Johnson V- and R-band filters were used during our observations. The typical exposure times for the V- and R-band filters is 800s and 600s, respectively. In all the observations, the sky flat-field frames in U, V and R passbands were obtained before and after each observation run during the twilight time.

The raw CCD images were preliminarily reduced through the standard CCDPROC routines in the IRAF package. For the purpose of differential photometry, we have first chosen several bright stars with good seeing from the same CCD frame as comparison stars. Then some check stars with brightness comparable to the object are selected to assess the errors in photometry. Aperture photometry is adopted to calculate the instrumental magnitudes of the objects and the selected stars by the APPHOT task in the IRAF package.

3 RESULTS AND DISCUSSIONS

3.1 Spectroscopic identification

The observed 1-dimensional spectra are visually classified into various types. The spectral types are listed in Column (12) in Table 1. All the observed sources are classified as stars except one AGN (i.e., GALEX J091332.6-101108.2). The spectrum of the object is shown in Figure 2. The spectrum of GALEX J091332.6-101108.2 shows a strong broad $H\alpha$ emission line, but a very weak and even undetectable broad $H\beta$ component, which allows us to classify the object as a Seyfert 1.9 galaxy rather than a typical type I AGN. The redshift is inferred to be $z=0.055$ according to the $H\alpha$ emission line. The continuum of the object is dominated by the stellar absorption features emitted from the host galaxy, which makes the object is not included in the quasar candidates selected from the GUVV2 catalog through their colors by Wheatley et al. (2008).

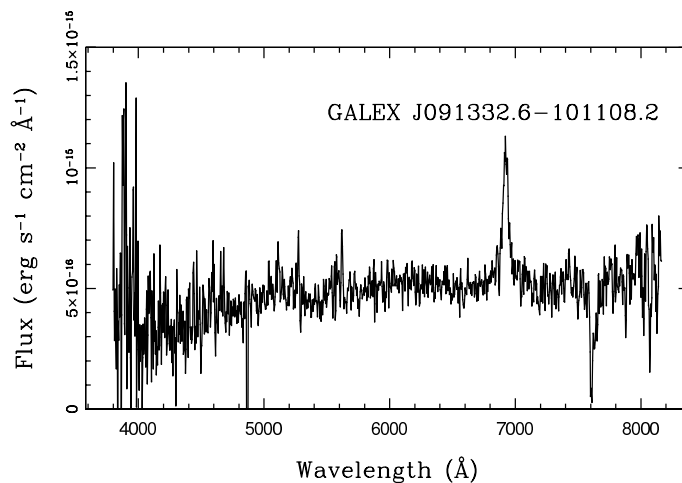


Fig. 2 Spectrum of the newly identified AGN: GALEX J091332.6-101108.2

GALEX NUV and FUV observation is found to be a sensitive probe for the variability of RR Lyare stars. The flux variability in RR Lyare stars is resulted from the radial pulsations that result in a cyclic temperature variation because of the stellar surface contraction and expansion. Out of the total 37 objects, 19 objects show spectra typical of type -A to -F stars since their strong Balmer absorption features and Balmer jumps. A typical spectrum is presented in Figure 3 as an illustration. Figure 4 shows the distribution of NUV magnitude variability for these identified type -A to -F stars. All the type -A to -F stars have large NUV magnitude variability. The average and median vaules is 1.22 and 1.20 magnitude, respectively, which is typical of the variability of RR Lyrae stars (Wheatley et al. 2005).

Seven M dwarf stars are identified in our spectroscopic observations. The spectra are present in Figure 5 for the 7 M dwarf stars. Five of them are active during our observations because of the detected $H\alpha$ emission line. M dwarf flare (dMe) stars are believed to be related with the coronal activity caused by their strong magnetic field coupled stellar disks (see review in Haisch et al. 1991). The flares last from seconds to hours in X-ray, ultraviolet, optical and radio bands (e.g., Schmitt et al. 1993; Phillips et al. 1998; Stepanov et al. 1995; Welsh et al. 2006). Although the physics of the flares is still poorly understood at present, it is widely believed that the UV flare emission in dMe is produced by the hot gas with temperature 10^5 K that are located at the chromosphere. In addition to the flare events, the coronal activity of dMe stars could be alternatively spectroscopic identified according to their strong Balmer emission lines, especially $H\alpha$ (e.g., Worden & Peterson 1976; Shkolnik et al. 2011).

Different from the other six M dwarf stars, the source (GALEX J123718.3+624207.9) shows a spectra of extreme early type ($\sim M0$) M dwarf star (see Fig.4). We here attempt to quantatively determined

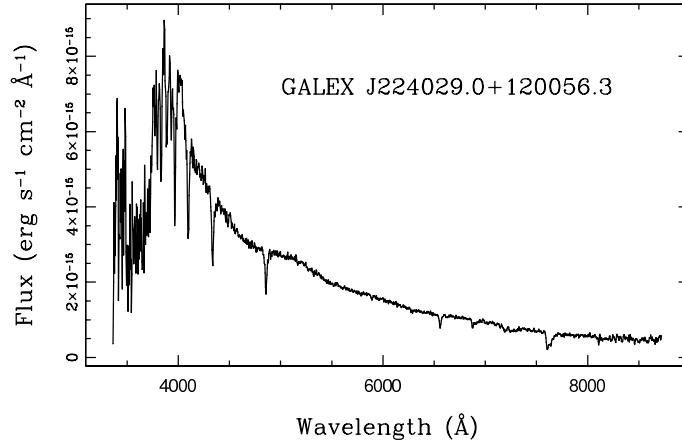


Fig. 3 A typical spectrum of newly identified A-type star.

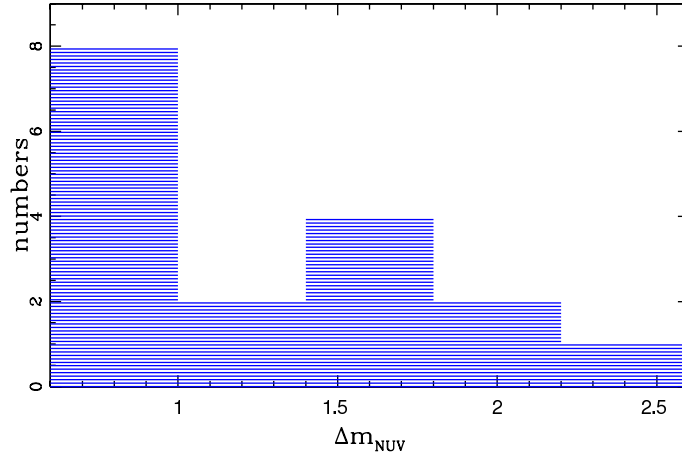


Fig. 4 Distribution of the Δm_{NUV} for the newly identified type -A to -F stars.

the spectral types for the other six M dwarf stars by already comprehensively studied spectral indices that are now widely used to produce quantitative spectral classification for M dwarfs according to their red part of the spectra (i.e., 6300-9000Å, e.g., Reid et al. 1995; Kirkpatrick et al. 1995; Martin et al. 1999; Hawley et al. 2002). Each index is defined as the ratio between the mean flux in the pseudo-continuum bands and molecular band. Taking into account of the spectral resolution of our spectra, the used spectral indices includes: TiO5, CaH2, CaH3 (Reid et al. 1995), TiO7140 (Wilking et al. 2005), VO2 (Lépine et al. 2003), and C81 (Stauffer et al. 1999). The values of the spectral indices are calculated for all the objects by using the *SPLIT* task in IRAF package, and are listed in Table 2. Our spectral type determination indicates that the spectral types calculated by different indices are generally consistent with each other within an uncertainty of about 1 sub-type for individual object. The determined average spectral types are listed in the last column in Table 2.

3.2 Cyclic light curves

Two RR Lyrae star candidates without spectroscopic identifications, GALEX J100133.2+014328.5 and GALEX J155800.6+535233.6, were monitored in optical V- and R-bands by us. Both light curves in R-

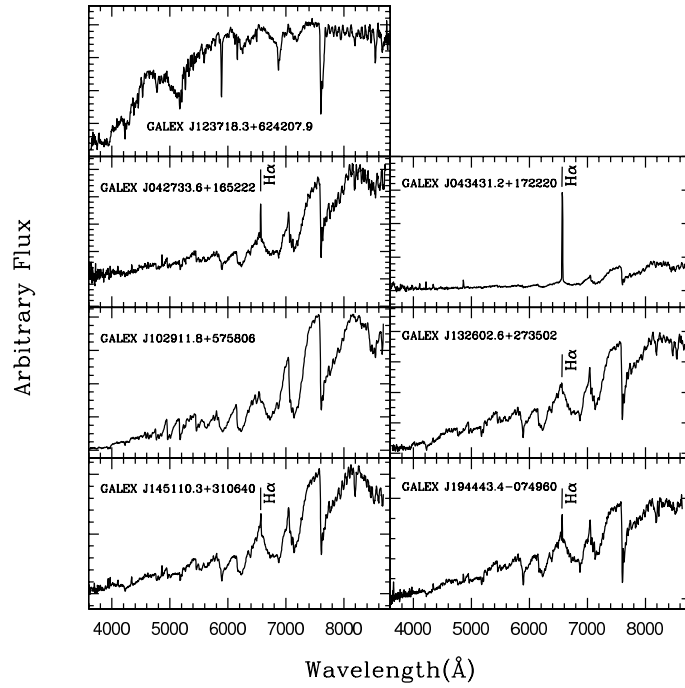


Fig. 5 Spectra of seven newly discovered M dwarf stars

Table 2 M dwarf stars: spectral types and corresponding spectral indices

GALEX Name	TiO 5	CaH 2	CaH 3	TiO 7140	VO 2	C81	Spectral type
GALEX J042733.6+165222	0.415	0.411	0.681	1.783	0.746	1.275	M3.78
GALEX J043431.2+172220	0.456	0.441	0.724	1.807	0.685	1.400	M3.70
GALEX J102911.8+575806	0.389	0.492	0.889	2.358	0.755	1.368	M3.61
GALEX J132602.6+273502	0.535	0.510	0.787	1.555	0.832	1.160	M2.63
GALEX J145110.3+310640	0.531	0.446	0.713	1.646	0.816	1.286	M3.22
GALEX J194443.4-074960	0.499	0.490	0.735	1.495	0.892	1.107	M2.71

band are presented in Figure 6. Cyclic variations can be identified from the light curves for both objects, although the light curves are under-sampling. For GALEX J100133.2+014328.5, the light curve in the first night covers not only the peak, which is confirmed by the observation in the next day, but also the followed valley. The PDM method yields a period roughly at 0.54 day. Given the light curve obtained in the first night, the R-band flux variability in the objects is as large as 1 mag, which is consistent with the typical value of RR Lyare stars (Skillen et al. 1993). Although the valley in the light curve is covered twice in GALEX J155800.6+535233.6, the peak in the light curve is missed in our observations because of the under-sampling. The poor sampling prevents us obtaining a period by the PDM method. The amplitude of NUV band of GALEX J100133.2+014328.5 and GALEX J155800.6+535233.6 are 1.98 and 0.87, respectively, which are far larger than the amplitude of the optical band. Combining the colors, cyclic light curves, and amplitude of ultraviolet and optical band allows us to classify the two objects as RR Lyare stars which preliminarily proof the result of the color-color diagram.

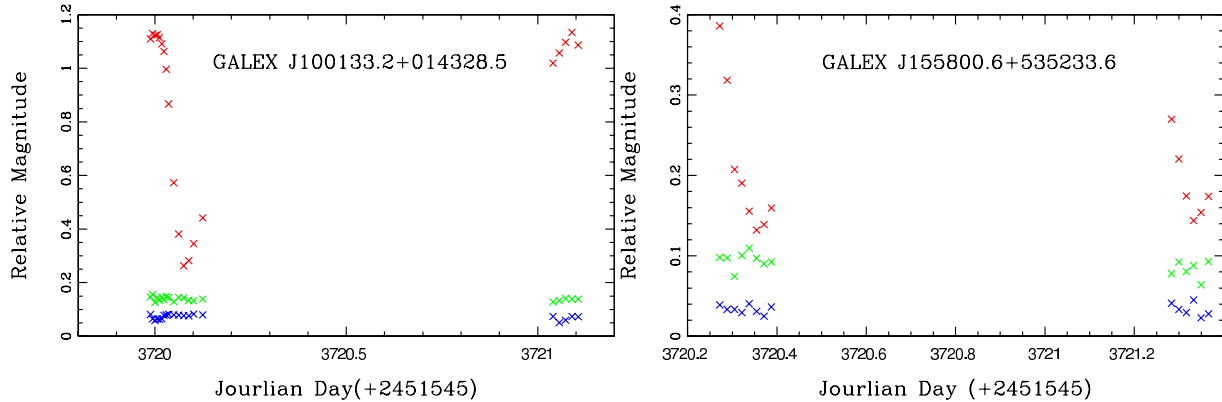


Fig. 6 Light curves of two RR Lyrae star candidates.

Table 3 Statistics of all the identified sources

AGNs (1)	RR Lyrae stars/Type A-F stars (2)	Type G-K stars (3)	M dwarf stars (4)	X-binaries (5)	Others (6)	Total (7)
78	25	10	9	19	9	150
52 %	16.7%	6.7%	6%	12.7%	6%	100%

Notes: Column (2) lists the previously identified RR Lyraes together with the newly identified type -A to -F stars.

3.3 Color-color diagram

In order to confirm the generality of the results derived from Figure 1, We compare the newly spectroscopically identified objects with the previously identified ones in the NUV-optical color-color diagram (Fig. 7). The newly identified type -A to -F stars, type -G to -K stars and M dwarf stars are marked as filled triangles with colors of green, yellow, and red, respectively.

The type -A to -F stars and M dwarf stars are clustered together with the previously identified RR Lyrae stars and M dwarf stars, respectively, which show good consistence with former results from Figure 1. Between the regions of type -A to -F stars and M dwarf stars, there gather some type -G to -K stars which may be solar-like coronal active stars, furtherly confirming the distribution trend of sources with different energy spectrum. The only one AGN marked as a large blue open star is classified as a Seyfert 1.9 galaxy, whose location is consistent with its continuum dominated by the stellar absorption features emitted from the host galaxy.

3.4 Statistics of the identified sources

There are totally 150 sources containing the newly spectroscopically identified and the sources with previously identifications. The statistics of all the identified sources with different types are listed in Table 3.

4 CONCLUSIONS

We have made a NUV-optical color-color plot for the previously known sources and the unidentified ones in GUVV2, which separate sources into different regions. The identified sources in each region corresponds to a certain spectral type, which allows us to tentatively classify the unknown sources simply by their NUV and optical magnitudes. In this method, we chosed two initially classified RR Lyrae star candidates to perform photometric monitors, there NUV and optical amplitude together with the cyclic light curves of which allows us to finally classify them as RR Lyrae stars. We have also carried out spectroscopic observations for 37 randomly chosen unknwn GUVV2 sources. There are seven M

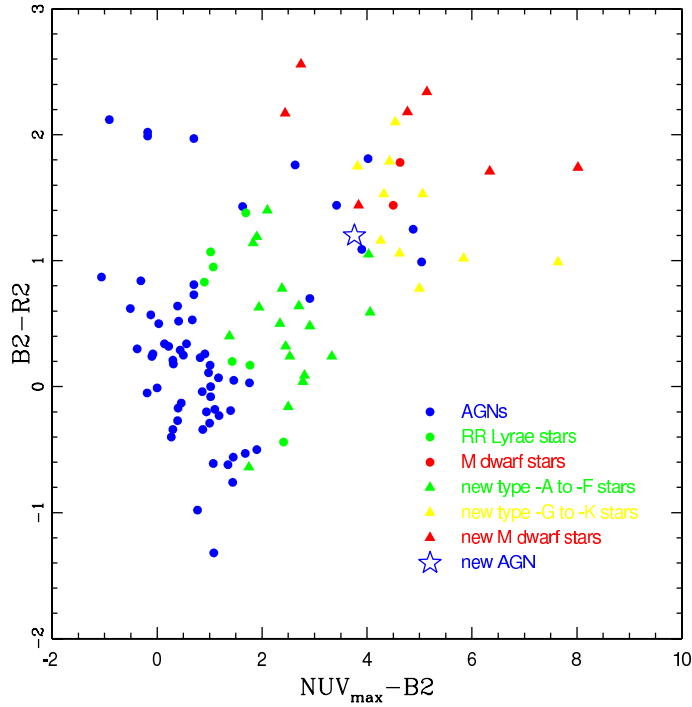


Fig. 7 Plot of $(NUV_{max} - B2)$ vs. $(B2 - R2)$ for the newly spectroscopically identified objects compared with the previously identified ones. The filled triangles with colors of green, yellow and red are newly discovered type -A to -F stars, type -G to -K stars and M dwarf stars; the large blue star is a newly discovered AGN. The previously identified sources are samely marked as Fig.6.

dwarf flare stars and an AGN. Five of the M dwarf stars are active during our observations because of their $H\alpha$ emission. The AGN shows a strong broad $H\alpha$ emission line, but a very weak and even undetectable broad $H\beta$ component, which allows us to classify the object as a Seyfert 1.9 galaxy rather than a typical type I AGN. The other sources are stars with spectral types from A to K. The location of all these newly identified sources on the NUV-optical diagram shows good consistence with the previously known sources, which confirm the correctness and generality of the initially classifications. Thus, at least for our results, we can rapidly and effectively classify the unknown ultraviolet variable sources into several spectral types by their NUV and optical magnitudes in advance.

Acknowledgements JW and JYW are supported by National Basic Research Program of China (Grant 2009CB824800). We would like to thank the anonymous referee for very useful comments and important suggestions that improved the presentation. This work was partially supported by the Open Project Program of the Key Laboratory of Optical Astronomy, NAOC, CAS. We thank Feng Qichen and Bai Yu for their share of observing time. Special thanks go to the staff at Xinglong observatory as a part of National Astronomical Observatories, China Science Academy for their instrumental and observational help.

References

Bianchi, L., et al. 2007, ApJS, 173, 659

- Browne, S. E. 2005, *PASP*, 117, 726
- Haisch, B., Strong, K. T., Rodono, M. 1991, *ARA&A*, 29, 275
- Hawley, S. L., et al. 2002, *AJ*, 123, 3409
- Kirkpatrick, J. D., Henry, T. J., & Simons, D. A. 1995, *AJ*, 109, 797
- Lépine, S., Rich, R. M., & Shara, M. M. 2003, *AJ*, 125, 1598
- Massey, P., Strobel, K., Barnes, J. V., & Anderson, E. 1988, *ApJ*, 328, 315
- Martín, E. L., Delfosse, X., Basri, G., Goldman, B., Forveille, T., & Zapatero Osorio, M. R. 1999, *AJ*, 118, 2466
- Martín, D. C., et al. 2005, *ApJ*, 619, 1
- Monet, D. G., et al. 2003, *AJ*, 125, 984
- Morrissey, P., et al. 2007, *ApJS*, 173, 682
- Phillips, K., Bromage, G., Dufton, P., et al. 1988, *MNRAS*, 235, 573
- Reid, I. N., Hawley, S. L., & Gizis, J. E. 1995, *AJ*, 110, 1838 (PMSU1)
- Schmitt, J., Haisch, B., & Barwig, H. 1993, *ApJ*, 419, 81
- Seibert, M., et al. 2005, *ApJ*, 619, L23
- Skillen, I., Fernley, J. A., Stobie, R. S., & Jameson, R. F. *MNRAS*, 265, 301
- Stepanov, A., Fuerst, E., Krueger, A., et al. 1995, *A&A*, 299, 739
- Shkolnik, E. L., Liu, M. C., Reid, I. N., Dupuy, T., & Weinberger, A. 2011, *ApJ*, 727, 6
- Stauffer, J. R., et al. 1999, *ApJ*, 527, 219
- Worden, S. P., & Peterson, B. M. 1976, *ApJ*, 206, 145
- Welsh, B. Y., et al. 2005, *AJ*, 130, 825
- Welsh, B. Y., et al. 2006, *A&A*, 458, 921
- Wheatley, J. M., et al. 2005 *ApJ*, 619, 123
- Wheatley, J. M., Welsh, B. Y., & Browne, S. E. 2008, *AJ*, 136, 259
- Wilking, B. A., Meyer, M. R., Robinson, J. G., & Greene, T. P. 2005, *AJ*, 130, 1733
- Zhou, A. Y., Jiang, X. J., Zhang, Y. P., & Wei, J. Y. 2009, *RAA*, 9, 349